

# Time-Dependent Stokes Shift and Its Calculation from Solvent Dielectric Dispersion Data

Chao-Ping Hsu, Xueyu Song,<sup>†</sup> and R. A. Marcus\*

A. A. Noyes Laboratory of Chemical Physics, 127-72, California Institute of Technology, Pasadena, California 91125

Received: October 8, 1996; In Final Form: January 13, 1997<sup>⊗</sup>

The time-dependent solvation correlation function (the *Stokes shift response function*), which describes the solvent response to a sudden change in the charge distribution of a solute molecule, is calculated here directly from experimentally measured dielectric dispersion data,  $\epsilon(\omega)$ , of the solvent. In the calculation a reaction field with the dielectric continuum assumption is used. This simple model is applied to the experimental results of Jimenez *et al.* for photoexcited coumarin and water as a solvent, and encouraging agreement is obtained using the experimental data on  $\epsilon(\omega)$ .

## 1. Introduction

The dynamics of polar solvents has been a topic of recent interest in physical chemistry and has frequently been studied in charge redistribution processes in many chemical reactions.<sup>1–20</sup> Experimentally, the time-dependent fluorescent shift (the *Stokes shift*) has been measured over different time scales and for a variety of polar solvents.<sup>2–8</sup> In typical Stokes shift experiments a chromophore solute in a polar solvent is first excited by a pump pulse, and then the time-dependent fluorescence spectrum of the solute is recorded. For studies with coumarin or other dye molecules (e.g., refs 3–8), the excited state of the solute has a different charge distribution from that in the ground state. There is expected to be little intramolecular vibrational motion excited when, as appears to be the case for some of these molecules, the geometry or vibration frequencies of the solute molecules are barely changed. In those cases, instead of vibrational Franck–Condon factors or of frictional effects due to a geometrical change of the solute (e.g., isomerization), the dynamics is dominated by the electrostatic interaction with the solvent, and then dielectric relaxation plays the major role in the relaxation process.

Recent theoretical developments<sup>9–20</sup> have provided physical insight into the solvation dynamics. Solvation correlation functions calculated from the Debye form, the Davidson–Cole, and the Cole–Cole forms were shown to exhibit significant differences.<sup>9</sup> On the basis of similar calculations and comparisons with experiments it was suggested that it would be useful to obtain higher frequency dielectric data for a better description of  $S(t)$ , the solvation correlation function.<sup>8</sup> The effect of molecular shape has also been discussed.<sup>10</sup> Much attention has also been devoted to treating the spatial dependence of the dielectric response function,  $\epsilon(\mathbf{k}, \omega)$ , which includes the molecular nature of the solvent.<sup>11,12</sup> The dynamical mean spherical approximation theory has been influential; the comparison with experimental results is at present qualitatively satisfactory.<sup>13,14</sup> A molecular hydrodynamic theory<sup>15,16</sup> has been applied to water solvation dynamics with a model dielectric response function.<sup>16,17</sup> Good agreement between the experimental and calculated solvation correlation function was obtained, and the role of the intermolecular O···O stretching mode was stressed.<sup>17</sup> Molecular dynamics calculations have provided information on how polar solvents change the reaction rate<sup>18</sup> and the role played by various shells of solvent molecules.<sup>9,19</sup> Such calculations

have also given results in satisfactory agreement with the dynamical Stokes shift experiments.<sup>7</sup> The short-time solvation dynamics has also been interpreted in terms of an *instantaneous normal modes* analysis of molecular dynamics simulations.<sup>20</sup> In another study, the ultrafast relaxation of the Stokes shift was related to the optical Kerr effect measurement using a Brownian oscillator model and assumptions on the spectral density<sup>21</sup> and showed an encouraging agreement for the description of fast dynamics of the solvent.

In the present work the time-dependent solvation correlation function is calculated using the entire dielectric spectral response function  $\epsilon(\omega)$ ,<sup>22</sup> instead of molecular models for the solvent. It will be seen that reasonable agreement with the experimental time-dependent Stokes shift is obtained using the measured  $\epsilon(\omega)$ <sup>23,24</sup> without explicitly considering the spatial dependence of dielectric relaxation, i.e.,  $\epsilon(\mathbf{k}, \omega)$ . The two solute–solvent models given in section 2 are dielectric continuum models with a dipole in a spherical cavity and an ellipsoid filled with dipole density,<sup>10,25</sup> with the induced charge on the boundary. The former is the usual *Onsager's cavity model*.<sup>26</sup> Comparison of these two models with each other and with the experimental results in ref 7 is given and discussed in section 3, followed by concluding remarks in section 4.

## 2. Calculation of the Solvation Correlation Function

The Stokes shift response function  $S(t)$  is defined in terms of the experimental measurements as

$$S(t) = \frac{\nu(t) - \nu(\infty)}{\nu(0) - \nu(\infty)} \quad (1)$$

where  $\nu(t)$  is the frequency of the fluorescence maximum at time  $t$ . If there is little internal vibrational excitation of the solute in the transition, then the time dependence of  $\nu(t)$  arises mainly from the time-dependent solvation energy,  $\Delta E^{\text{solv}}(t)$ , resulting from the change in the charge distribution of solute induced by the photoexcitation at  $t = 0$ .  $S(t)$ , also termed a “solvation correlation function”, can be rewritten as

$$S(t) = \frac{\Delta E^{\text{solv}}(t) - \Delta E^{\text{solv}}(\infty)}{\Delta E^{\text{solv}}(0) - \Delta E^{\text{solv}}(\infty)} \quad (2)$$

In the following section  $\Delta E^{\text{solv}}(t)$  is related to the dielectric dispersion  $\epsilon(\omega)$  by assuming that the solvation energy is the electrostatic interaction energy between the solute and the surrounding solvent.

<sup>†</sup> Present address: Department of Chemistry, University of California, Berkeley, CA 94720.

<sup>⊗</sup> Abstract published in *Advance ACS Abstracts*, March 1, 1997.

**2.1. Dielectric Continuum Models.** For the case where the charge distribution of the solute is a point dipole moment,  $\mu$ , the energy of interaction of the dipole with the solvent,  $E^{\text{solv}}(t)$ , is

$$E^{\text{solv}}(t) = -\mu(t) \cdot \mathbf{R}(t) \quad (3)$$

where  $\mathbf{R}(t)$  is the reaction field at time  $t$  due to the surrounding solvent acting on the solute dipole. The reaction field  $\mathbf{R}(t)$  can be obtained from linear response theory:

$$\mathbf{R}(t) = \int_{-\infty}^t dt' \mathbf{r}(t-t') \mu(t') \quad (4)$$

where  $\mathbf{r}(t-t')$  is a response function and, in general, is a tensor. Causality requires that  $\mathbf{r}(t) = 0$  for  $t < 0$ . The Fourier transform is introduced

$$\tilde{f}(z) = \int_{-\infty}^{\infty} dt f(t) e^{-izt} \quad (5)$$

where  $z$  can be generalized to be a complex variable. Usually there is a range for  $\text{Im}(z)$  where  $\tilde{f}(z)$  is analytic.<sup>27</sup> The inverse of eq 5 is given by the standard expression

$$f(t) = \frac{1}{2\pi i} \int_C dz e^{izt} \tilde{f}(z) \quad (6)$$

where  $C$  is a suitable contour that goes from  $-\infty$  to  $\infty$  if projected onto the real axis and stays inside the region where  $\tilde{f}(z)$  is analytic. Using the convolution theorem, eq 4 yields

$$\tilde{\mathbf{R}}(z) = \tilde{\mathbf{r}}(z) \tilde{\mu}(z) \quad (7)$$

We consider now a model system where it is assumed that the solute is treated as a spherical cavity with the dipole placed at the center. To obtain the appropriate equation for  $\tilde{\mathbf{r}}(z)$ , both for this model of the solute and for any other, it is necessary to solve the time-dependent electrostatic problem for the system. The dielectric displacement,  $\mathbf{D}_i$ , in any phase  $i$  is related to the electric field there,  $\mathbf{E}_i$ , and the dielectric polarization  $\mathbf{P}_i$  by<sup>28</sup>

$$\mathbf{D}_i(\mathbf{r}, t) = \mathbf{E}_i(\mathbf{r}, t) + 4\pi \mathbf{P}_i(\mathbf{r}, t) \quad (8)$$

where there should be no danger of confusing the position coordinate  $\mathbf{r}$  in eqs 8–12 and in footnote 30 with the linear response function  $\mathbf{r}$  in eq 4.

In linear response theory,

$$\mathbf{P}_i(\mathbf{r}, t) = \int_{-\infty}^t dt' \alpha_i(t-t') \mathbf{E}_i(\mathbf{r}, t') \quad (9)$$

where it is assumed that the polarizability of the region  $\alpha_i$  is local in space. For a two-phase system,  $i = 1, 2$ , the boundary conditions at the (1,2) interface are that the normal components  $\mathbf{D}_i^\perp(\mathbf{r}, t)$  are equal when there is no interfacial charge density, and the parallel components  $\mathbf{E}_i^\parallel(\mathbf{r}, t)$  are also equal.<sup>29</sup> Taking the Fourier transform of eq 9 and of these boundary conditions, we have<sup>30</sup>

$$\tilde{\mathbf{P}}_i(\mathbf{r}, z) = \tilde{\alpha}_i(z) \tilde{\mathbf{E}}_i(\mathbf{r}, z) \quad (10)$$

and

$$\tilde{\mathbf{D}}_1^\perp(\mathbf{r}, z) = \tilde{\mathbf{D}}_2^\perp(\mathbf{r}, z), \quad \tilde{\mathbf{E}}_1^\parallel(\mathbf{r}, z) = \tilde{\mathbf{E}}_2^\parallel(\mathbf{r}, z) \quad (11)$$

From eq 10 we have

$$\tilde{\mathbf{D}}_i(\mathbf{r}, z) = \epsilon_i(z) \tilde{\mathbf{E}}_i(\mathbf{r}, z), \quad i = 1, 2 \quad (12)$$

where the frequency-dependent dielectric constant  $\epsilon_i(z)$  is

$$\epsilon_i(z) = 1 + 4\pi \tilde{\alpha}_i(z), \quad i = 1, 2 \quad (13)$$

Equations 11 and 12 are the same as the static equations, and so the solution of the static boundary value problem applies here. Using the standard reaction field expression,<sup>25,31</sup> one thus obtains for the case of a point dipole in a sphere,

$$\tilde{r}(z) = \frac{2}{a^3} \frac{\epsilon(z) - 1}{2\epsilon(z) + 1} \quad (14)$$

where  $a$ , the radius of the cavity, represents the size of the solute. Since a normalization appears in calculating  $S(t)$  in eq 2, any constant factor cancels, and so the final response function is independent of  $a$ . Equations 7 and 14, with  $z$  replaced by  $\omega$ , were used in ref 31 and termed there a *quasi-static boundary-value* calculation. An explicit derivation of the equations is given above, and the method can be applied to any other model for the solute.

We consider the case where the optical excitation of the solute molecule occurs, in effect, instantaneously and the dipole moment of the molecule is changed from  $\mu_g$  to  $\mu_e$  at time  $t = 0$ . Thus, the dipole moment of the solute  $\mu(t)$  can be written as

$$\mu(t) = \mu_g + \theta(t)(\mu_e - \mu_g) \quad (15)$$

where  $\theta(t)$  is the unit step function. Therefore, eq 4 yields

$$\mathbf{R}(t) = r_s \mu_g + \int_{-\infty}^t dt' r(t-t') \theta(t') \Delta\mu \quad (16)$$

where, using eq 14,<sup>32</sup>

$$r_s \equiv \tilde{r}(0) = \int_{-\infty}^t dt' r(t-t') = \frac{2}{a^3} \frac{\epsilon_s - 1}{2\epsilon_s + 1} \quad (17)$$

Here,  $\Delta\mu \equiv \mu_e - \mu_g$  and  $\epsilon_s$  is the static dielectric constant of the solvent. The first term in eq 16 describes the reaction field arising from  $\mu_g$ , and the second term is the change in  $\mathbf{R}(t)$  due to the sudden change of dipole at time  $t = 0$ . The former equals the static reaction field  $r_s \mu_g$ , since before the excitation the solvent is in equilibrium with the ground state dipole moment.

At time  $t$ , if the molecule suddenly fluoresces, and so reverts to the ground state, the dipole moment is changed back to  $\mu_g$  and the solvent has an immediate reaction arising from the optical frequency dielectric constant,  $\epsilon_{\text{op}}$ . If  $\mathbf{R}_f(t)$  denotes the reaction field immediately after this instantaneous reaction of the solvent, then

$$\mathbf{R}_f(t) = \mathbf{R}(t) - r_{\text{op}} \Delta\mu \quad (18)$$

where  $\mathbf{R}(t)$  is the value just prior to this fluorescence, given by eq 16, and

$$r_{\text{op}} = \frac{2}{a^3} \frac{\epsilon_{\text{op}} - 1}{2\epsilon_{\text{op}} + 1} \quad (19)$$

The resulting solvation energy difference between the excited state and the ground state molecule, at time  $t$ , is now

$$\begin{aligned} \Delta E^{\text{solv}}(t) &= E_e^{\text{solv}}(t) - E_g^{\text{solv}}(t) = -\mu_e \cdot \mathbf{R}(t) + \mu_g \cdot \mathbf{R}_f(t) \\ &= -\mu_g \cdot (r_{\text{op}} + r_s) \Delta\mu + \Delta E(t) \end{aligned} \quad (20)$$

where

$$\Delta E(t) = -(\Delta\mu)^2 \int_{-\infty}^t dt' r(t-t') \theta(t') \quad (21)$$

In eq 20, only the second term is time-dependent and so the first term cancels in calculating  $S(t)$  in eq 2.

The Fourier transform of  $\Delta E(t)$  can be obtained using the complex Fourier transform of  $\theta(t)$ ,

$$\int_{-\infty}^{\infty} \theta(t) e^{-izt} dt = \left[ \frac{e^{-izt}}{-iz} \right]_{t=0}^{\infty} = \frac{1}{iz}, \quad \text{if } \text{Im}(z) < 0 \quad (22)$$

Therefore, from the convolution theorem,

$$\Delta \tilde{E}(z) = -\frac{(\Delta\mu)^2}{iz} \tilde{r}(z) \quad (23)$$

where  $z$  denotes  $(\omega - i\eta)$  with  $\omega$  real and  $\eta$  being a small positive number.<sup>33</sup> Taking the inverse transform of  $\Delta \tilde{E}(z)$ , we have, using the results in Appendix A,

$$\begin{aligned} \Delta E(t) &= -\frac{(\Delta\mu)^2}{2\pi} \int_C dz e^{izt} \frac{1}{iz} \tilde{r}(z) \quad (24) \\ &= -\frac{4(\Delta\mu)^2}{a^3\pi} \int_0^{\infty} d\omega \frac{\cos \omega t}{\omega} \text{Im} \left[ \frac{\epsilon(\omega) - 1}{2\epsilon(\omega) + 1} \right] - (\Delta\mu)^2 r_s, \end{aligned}$$

for  $t \geq 0$  (25)

The contour of integration,  $C$ , in eq 24 denotes a path parallel to but slightly below the real axis in the complex  $z$  plane. The solvation correlation function  $S(t)$  can be calculated using eqs 2, 20, and 25. The optical response has already been included in eq 18, and so the  $\infty$  in eq 25 actually denotes a high frequency,  $\omega_{\text{op}}$ , below the optical absorption band and the  $\text{Im} \epsilon(\omega)$  is essentially zero at  $\omega_{\text{op}}$ . The integration over  $z$  in eq 24 is discussed in Appendix A, and remarks on the relation between the optical response and the upper limit of the frequency range of eq 25 are made in Appendix B.

The effect of molecular shape was also studied here by considering an ellipsoid model: if an ellipsoid filled with homogeneous dipole density is used to represent the solute, the solution for the reaction field  $\mathbf{R}$  is given in section 20 of ref 25 and in ref 10. For any frequency  $\omega$ , it is the same as in eq 7 except for a different response function  $\tilde{\mathbf{r}}(\omega)$ :

$$\tilde{\mathbf{r}}(\omega) = \begin{pmatrix} f_a & 0 & 0 \\ 0 & f_b & 0 \\ 0 & 0 & f_c \end{pmatrix} \quad (26)$$

where

$$f_i = \frac{3}{abc} \frac{A_i(1 - A_i)[\epsilon(\omega) - 1]}{\epsilon(\omega) + [1 - \epsilon(\omega)]A_i}, \quad i = a, b, c \quad (27)$$

and  $A_a, A_b$ , and  $A_c$  are ellipsoidal shape factor integrals.<sup>25</sup> Tables and the relation of these shape factors to elliptic functions are given in ref 34. The expression for the solvation energy ( $\Delta E^{\text{solv}}(t)$ ) is similar to that in eq 20 except that now  $\mathbf{r}$  is a tensor instead of a scalar  $r$ :

$$\Delta E(t) = \Delta\mu \cdot \int_{-\infty}^t dt' \mathbf{r}(t-t') \theta(t') \cdot \Delta\mu \quad (28)$$

The expression for  $\Delta \tilde{E}(z)$  given by eq 23 becomes

$$\Delta \tilde{E}(z) = -\frac{1}{iz} \Delta\mu \cdot \tilde{\mathbf{r}}(z) \cdot \Delta\mu \quad (29)$$

The inverse Fourier transform of this equation yields  $\Delta E(t)$ :

$$\Delta E(t) = -\frac{2}{\pi} \Delta\mu \cdot \int_0^{\infty} d\omega \frac{\cos \omega t}{\omega} \text{Im} \tilde{\mathbf{r}}(\omega) \cdot \Delta\mu - \Delta\mu \cdot \tilde{\mathbf{r}}(0) \cdot \Delta\mu \quad (30)$$

which is then used to calculate  $S(t)$ . If the above expressions are applied to a *sphere* filled with homogeneous dipole density ( $A_a = A_b = A_c = 1/3$ ), the expression for  $\Delta E(t)$  is the same as that given by eq 25 for the dipole in a sphere model.

**2.2. Results.** The above models are now applied to the system of coumarin 343 (C343) dissolved in water.<sup>7</sup> The results of a numerical calculation, using eqs 2, 20, and 25 and the  $\epsilon(\omega)$  of water at  $T = 298$  K,<sup>23,24</sup> are plotted in Figure 1. As in ref 22, in the low-frequency region ( $\omega \leq 3.0 \times 10^{11}$  rad s<sup>-1</sup>, about 1.6 cm<sup>-1</sup>),<sup>35</sup> Debye's formula is used,

$$\epsilon(\omega) = \epsilon_i + \frac{\epsilon_s - \epsilon_i}{1 + i\omega\tau_D} \quad (31)$$

with  $\tau_D = 8.2$  ps,  $\epsilon_s = 78.3$ , and  $\epsilon_i = 4.21$ . For the frequency range  $\omega = 3.0 \times 10^{11}$  to  $7.2 \times 10^{14}$  rad s<sup>-1</sup>, a spline fit was used for both the real and imaginary parts of  $\epsilon(\omega)$ . The upper limit of the integration is  $7.2 \times 10^{14}$  rad s<sup>-1</sup>, which is approximately 3800 cm<sup>-1</sup>. The optical dielectric constant ( $\epsilon_{\text{op}}$ ) was assumed to be 1.8. The same numerical answer was obtained for the integration in eq 25 using either the fast Fourier transform (FFT) subroutines or the direct numerical integration. This agreement confirms the quality of the present calculation. The plot of the calculated  $S(t)$  is compared in Figures 1 and 2 with the  $S(t)$  obtained from the experimentally fitted parameters of experimental data in ref 7.

For an oblate ellipsoid with  $a/b = a/c = 0.4$  and with the change of dipole  $\Delta\mu$  parallel to one of the long axes,  $\Delta E(t)$  was calculated by the inverse Fourier transform of eq 29 and then  $S(t)$  is obtained from eqs 2 and 20. The dimensions of the ellipsoid were chosen to approximate the shape of the coumarin ion.<sup>4</sup> For this case the ellipsoidal shape factors are<sup>34</sup>  $A_a = 0.588$ ,  $A_b = A_c = 0.206$ . The results of the calculation are plotted in Figure 2.

### 3. Discussion

We see from Figures 1 and 2 that this simple continuum model of solute and solvent gives a time-dependent Stokes shift reasonably close to that observed in the experiment. There may or may not be a difference of behavior at very short times ( $\sim 50$  fs) in Figure 1 between the experimental and calculated curves. In the experiments,<sup>7</sup> the cross-correlation of the pump pulse and the gate pulse is reported to be 100–110 fs (full width at half-maximum).

It is perhaps surprising that the simple model works as well as it does, and it will be interesting to see whether similar agreement is obtained for other solvents. Because the dielectric dispersion  $\epsilon(\omega)$  of the solvent contains a broad range of frequencies in its response, it is not surprising that the calculated response function, like the experimental, is far from being a single exponential. The entire dielectric dispersion spectrum of  $\epsilon(\omega)$  includes the low-frequency part, which is well-described by the Debye formula, and the high-frequency part, which contains various contributions from inter- and intramolecular vibrational modes of the solvent. The former contributes to the long-time behavior, whose characteristic behavior is diffusional, while the latter is more "reversible" and determines the short-time behavior.

Many studies on solvation dynamics (e.g., refs 5, 8–10, 14, 17, 31, 39–41) use an analytic form for  $\epsilon(\omega)$  which includes various models for the low-frequency part and damped oscillations for higher frequency region. Hornig *et al.*<sup>5</sup> has included

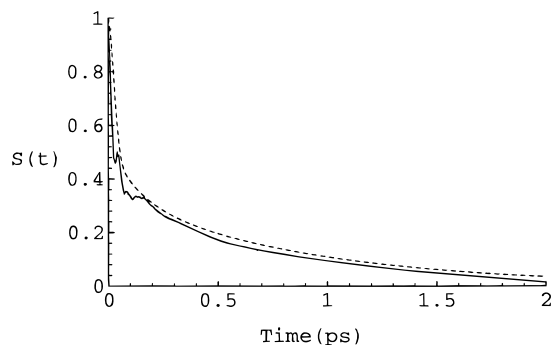


**Figure 1.** Calculated  $S(t)$  (solid line) for a dipole in a sphere using eq 25. The dashed line depicts the experimental result from ref 7. The latter is a fit to their experimental data with one narrow Gaussian and two exponential functions.

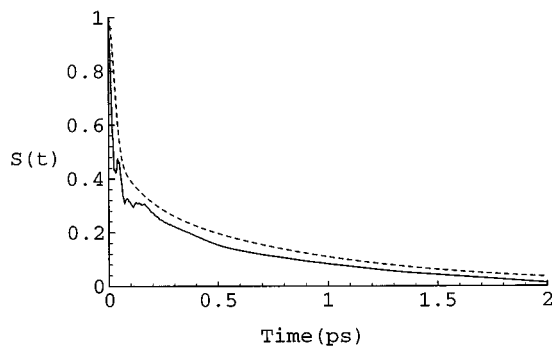


**Figure 2.** Calculated  $S(t)$  (solid line) for a model of an ellipsoid solute using eqs 26 and 29. The ellipsoid has  $a:b:c = 0.4:1:1$  with the dipole moment lying on the  $b$  or  $c$  axis. The dashed line is the experimental result, which is the same as that in Figure 1.

a low-frequency Debye model and two or three damped oscillators at higher frequencies for acetonitrile and methanol and has obtained a reasonably good  $S(t)$  for acetonitrile. In the interesting work by Nandi *et al.*<sup>17</sup> excellent agreement between the experimental and calculated  $S(t)$  was obtained, although the model provided for water did not quite resemble the experimental  $\epsilon(\omega)$ . Loring *et al.*<sup>39</sup> calculated the fluorescence and hole-burning line shape with a molecular theory using a Debye model for  $\epsilon(\omega)$  in obtaining the results. Jarzaba *et al.*<sup>8</sup> showed that simple continuum models, such as single- or multiple-component Debye models or the Cole–Davidson model, accurately predicted the averaged solvation time but not the shape of  $S(t)$ , and they suggested that it would be useful to have higher frequency dielectric data included. Their suggestion is indeed confirmed by our present calculation.

We used a spline fit for the discrete data of  $\epsilon(\omega)$ . Thereby, there were no adjustable parameters and a direct connection was made between  $\epsilon(\omega)$  and  $S(t)$ . Any analytical model that provides a reasonably good description of the  $\epsilon(\omega)$  spectrum would of course give essentially the same  $S(t)$ . However, we believe that directly using the experimental dielectric dispersion data with a simple continuum model provides a transparent way of introducing the solvation dynamics, especially for the possible cases where model dielectric theories do not provide a satisfactory description of  $\epsilon(\omega)$ .

The model used in Figure 1 is the dipole in a spherical cavity in a solvent dielectric continuum, while that used in Figure 2 is the ellipsoid with a homogeneous dipole density. The rate of decay of  $S(t)$  with  $t$  for the latter is slightly faster than that for the former. There is seen to be little effect of changing the shape of solute from a sphere to an ellipsoid. Results (not shown) were also obtained for the  $S(t)$  when the dipole is replaced by a single charge. In that case, the solvent response

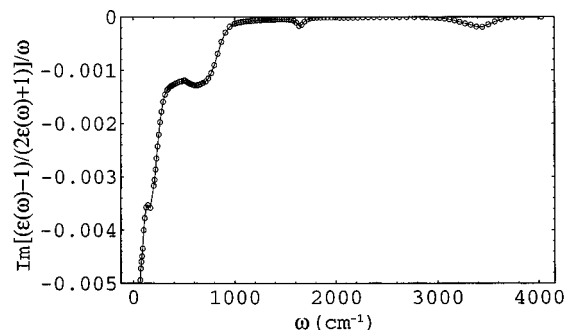


**Figure 3.** Imaginary part of the quantity  $[(\epsilon(\omega) - 1)/(2\epsilon(\omega) + 1)]/\omega$  which is proportional to the term that is cosine transformed in eq 25, for the dipole in a sphere cavity. Circles denote the data points calculated from experimental  $\epsilon(\omega)$ . The zero-frequency limit of this quantity, estimated from the Debye formula (eq 31), is  $-0.073 \text{ ps rad}^{-1}$ . It is seen that the contribution of the intramolecular vibrational bands is quite small compared to that of the librational mode at about  $800 \text{ cm}^{-1}$ . The units of the ordinate are  $\text{ps rad}^{-1}$ .

$r(\omega)$  in eq 14 is replaced by  $1 - 1/\epsilon(\omega)$ . One then finds that the results in Figure 2 for the ellipsoid filled with a uniform dipole density lie between those for the dipole in a sphere in Figure 1 and those for a charge in a sphere. This result is not unexpected, since the ellipsoid filled with a homogeneous dipole density that is parallel to the long axis has net charges distributed at the surface at both ends of the long axis. The latter would behave more or less like two not quite separated regions of charge density and would be intermediate between a charge and a point dipole in its behavior.

In the results of the present calculation, the small peaks of recurrence in Figures 1 and 2 show a “reversibility” of the motion, with the shortest period being about 44 fs, which corresponds to roughly  $760 \text{ cm}^{-1}$  in frequency. The absorption band in that region has been assigned to a “libration”, namely, oscillation of the water molecule in the force field of its neighbors.<sup>25</sup> The other bands with higher frequencies in  $\epsilon(\omega)$  do not yield any significant recurrence from the rapid initial decay of  $S(t)$ , due to their contribution to  $\epsilon(\omega)$  being very small and, to a lesser extent, due to the  $1/\omega$  factor in the integrand. Thereby, these resonance bands contribute only a small portion of the rapid initial decay (cf. Figure 3). Nandi *et al.*<sup>17</sup> pointed out the importance of the intermolecular O···O stretching mode, which constitutes the  $193 \text{ cm}^{-1}$  band in  $\epsilon(\omega)$  and corresponds to 170 fs as its recurrence period. In Figure 3 there is a small shoulder located between  $150$  and  $200 \text{ cm}^{-1}$  arising from such motion. In Figures 1 and 2, the (broader) recurrence peak at about 0.2 ps can be regarded as a mixed result of this lower frequency band and the librational motion, and the rate of decay is seen to slow down at this region, for both the experimental and the calculated  $S(t)$ .

A molecular dynamics (MD) simulation of rigid water showed a similar pattern of recurrence in  $S(t)$ <sup>7</sup> and supports the idea that the principal reversible mode is intermolecular. In that MD work the amount of initial decay is, out of the total calculated  $S(t)$ , roughly 10% less than our result in Figure 1. Part of this difference may arise from the effect of the rapidly dephased intramolecular modes of water, which occurs in our calculation: It includes all dispersive contributions, unlike the MD result, since a rigid model for the individual water molecules was used in the latter. Both the MD study and the present result show the importance of including the moderately high frequency intermolecular components of the dielectric response spectrum on the dynamics in sub-picosecond time scale, in addition to including the Debye region.

In Figures 1 and 2 it is seen that  $S(t)$  for an oblate ellipsoid with its dipole “lying” in the plane of the molecule decays only

slightly faster than it does for a sphere. Recalling that the sphere model also applied to a homogeneous dipole density model, we also see in this comparison that the molecular shape affects  $S(t)$  only a little, within the approximation of using a dielectric continuum. For a more complete description of the solvation dynamics, in addition to satisfying the boundary condition at the solute–solvent interface, the spatial dependence of the dielectric constant<sup>11,36</sup> would also be taken into account.

When the smooth decay of our theoretically calculated  $S(t)$  after 0.5 ps is fitted by an exponential function, the results in Figure 1 correspond to a lifetime of 810 fs. This number agrees well with the slowest exponential component in ref 7 obtained by fitting to the experimental data, namely, 880 fs. On the other hand, the Debye model (eq 31) describes a single-exponential relaxation process: For the sphere cavity model, the relaxation time for  $S(t)$  obtained from the Debye formula is  $\tau_D(2\epsilon_i + 1)/(2\epsilon_s + 1)$  (e.g., ref 31), which is 490 fs. The Debye model is a good description of  $\epsilon(\omega)$  for  $\omega = 0$  to about  $3.0 \times 10^{11}$  rad  $s^{-1}$ . For frequencies higher than that, the measured  $\epsilon(\omega)$  begins to deviate from Debye's formula. Thereby, a decay occurring according to the Debye formula is expected to occur only after 3 ps. The current lifetime fit for  $t = 0.5$ – $2$  ps is not, we have just seen, the Debye 490 fs and represents a mixed result from both the Debye model and the spline fit of dielectric dispersion for higher frequencies.

#### 4. Conclusion

The solvation correlation function can be calculated by including the entire spectrum of dielectric dispersion data  $\epsilon(\omega)$  up to the optical region. Using simple dielectric continuum models that neglect the molecular property of the solvent, our results show that the correlation function obtained gives a reasonable description for the time-dependent Stokes shift measurement.

**Acknowledgment.** It is a pleasure to acknowledge the support of this research by the National Science Foundation and by the Office of Naval Research. This article is dedicated to the memory of a long-time friend, Heinz Gerischer, whom one of us had the pleasure of knowing for almost 40 years. Heinz was a generous and thoughtful individual whose impact on electrochemistry is enormous.

#### Appendix A: Analysis for Equation 24

Equation 24 can be rewritten as

$$\Delta E(t) = -\frac{\Delta\mu^2}{2\pi} \int_C dz \frac{\tilde{r}(z)}{iz} e^{izt} \quad (\text{A1})$$

$$= -\frac{\Delta\mu^2}{2\pi} \int_C dz \frac{\tilde{r}(z) - \tilde{r}(0)}{iz} e^{izt} - \frac{\Delta\mu^2}{2\pi} \int_C dz \frac{\tilde{r}(0)}{iz} e^{izt} \quad (\text{A2})$$

where  $C$  denotes a contour that is parallel but slightly below the real axis. The second of the integrals in eq A2 can be shown, using the residue theorem, to equal  $2\pi\tilde{r}(0)\theta(t)$ . We note that  $\tilde{r}(z)$  is analytic on the real axis,<sup>33</sup> and  $\tilde{r}(z=0)$  is a real number.<sup>32</sup> The integrand in the first integral does not possess a pole at  $z = 0$ , since

$$\frac{\tilde{r}(z) - \tilde{r}(0)}{z} = \left[ \frac{d\tilde{r}(z)}{dz} \right]_{z=0} + O(z), \quad z \rightarrow 0 \quad (\text{A3})$$

and  $d\tilde{r}(z)/dz$  has no singularity at  $z = 0$ . We may therefore allow the contour  $C$  for the first integral in eq A2 to coincide with the real axis. Denoting the real and imaginary part of  $\tilde{r}(\omega)$

by  $\tilde{r}'(\omega)$  and  $\tilde{r}''(\omega)$ , respectively, i.e.,  $\tilde{r}(\omega) = \tilde{r}'(\omega) + i\tilde{r}''(\omega)$ , and noting that  $\tilde{r}(-\omega) = \tilde{r}^*(\omega)$ , which follows because  $r(t)$  is real, we then find

$$\int_C dz \frac{\tilde{r}(z) - \tilde{r}(0)}{iz} e^{izt} = 2 \int_0^\infty d\omega \frac{\tilde{r}''(\omega)}{\omega} \cos \omega t + 2 \int_0^\infty d\omega \frac{\tilde{r}'(\omega) - r_s}{\omega} \sin \omega t \quad (\text{A4})$$

Therefore, eq A2 yields

$$\Delta E(t) = -\frac{\Delta\mu^2}{\pi} \left[ \int_0^\infty d\omega \frac{\tilde{r}''(\omega)}{\omega} \cos \omega t + \int_0^\infty d\omega \frac{\tilde{r}'(\omega) - r_s}{\omega} \sin \omega t + \pi r_s \theta(t) \right] \quad (\text{A5})$$

Another useful property is obtained by noting that  $\Delta E(t) = 0$  for  $t < 0$  (eq 21). The first integrand in eq A5 is an even function of  $t$ , while the second is an odd function. Since the sum of them yields zero for negative  $t$ , they must be equal for positive  $t$ . Thus, the calculation for  $\Delta E(t)$  can be performed by integrating either of the two terms in eq A5. In the present work, the first term was used because  $\tilde{r}''(\omega)$  goes to zero as  $\omega$  goes to the optical limit in an integration region, and so it is numerically easier to calculate. We can write

$$\Delta E(t) = -\frac{2\Delta\mu^2}{\pi} \int_0^\infty d\omega \frac{\tilde{r}''(\omega)}{\omega} \cos \omega t - \Delta\mu^2 r_s, \quad \text{for } t \geq 0 \quad (\text{A6})$$

which yields eq 25.

The second term of eq (A5) can be better evaluated, if desired, as follows,

$$\int_0^\infty d\omega \frac{\tilde{r}'(\omega) - r_s}{\omega} \sin \omega t = \int_0^\infty d\omega \frac{\tilde{r}'(\omega) - r_{op}}{\omega} \sin \omega t + \int_0^\infty d\omega \frac{r_{op} - r_s}{\omega} \sin \omega t \quad (\text{A7})$$

$$= \int_0^\infty d\omega \frac{\tilde{r}'(\omega) - r_{op}}{\omega} \sin \omega t + \pi \left( \theta(t) - \frac{1}{2} \right) (r_{op} - r_s) \quad (\text{A8})$$

The first term now has a finite range of  $\omega$  and so is numerically easier to calculate than the left-hand side of eq A7.

#### Appendix B: Remark on the Optical Response Contribution

At time  $t = 0$ , the first term in eq A6 would formally become

$$-\frac{2\Delta\mu^2}{\pi} \int_0^\infty d\omega \frac{\tilde{r}''(\omega)}{\omega} = \Delta\mu^2 \tilde{r}''(0) = \Delta\mu^2 r_s \quad (\text{B1})$$

Equation B1 follows from the Kramers–Kronig relationship<sup>37,38</sup> when the upper limit is really  $+\infty$  (and not  $\omega_{op}$ ). Equation A5 then gives  $\Delta E(0) = 0$ . However, practically the integration is cut off at a frequency ( $\omega_{op}$ ) in the range between the response arising from nuclear motions ( $0 < \omega < \omega_v$ ) and the electronic polarization ( $\omega_{el} < \omega < \infty$ ). Because of the large separation of the two frequency regions (e.g.  $\omega_v \approx 10^3$   $\text{cm}^{-1}$  while  $\omega_{el} \approx 10^5$   $\text{cm}^{-1}$ ), the  $\tilde{r}''(\omega)$  from the fast electronic polarization gives approximately a constant contribution  $r_{op}$  to  $\tilde{r}'(\omega)$  over the lower frequency region ( $0 < \omega < \omega_v$ ).<sup>38</sup> That constant can be obtained from the Kramers–Kronig relation:

$$r_{\text{op}} = \tilde{r}'(\omega_{\text{op}}) = \frac{2}{\pi} P \int_0^{\infty} d\omega \frac{\omega \tilde{r}''(\omega)}{\omega_{\text{op}}^2 - \omega^2}$$

$$\approx \frac{2}{\pi} \left[ \int_0^{\omega_{\text{v}}} d\omega \frac{\omega \tilde{r}''(\omega)}{\omega_{\text{op}}^2 - \omega^2} + \int_{\omega_{\text{el}}}^{\infty} d\omega \frac{\omega \tilde{r}''(\omega)}{\omega_{\text{op}}^2 - \omega^2} \right] \quad (\text{B2})$$

$$\approx 0 - \frac{2}{\pi} \int_{\omega_{\text{el}}}^{\infty} d\omega \frac{\tilde{r}''(\omega)}{\omega} \approx - \frac{2}{\pi} \int_{\omega_{\text{op}}}^{\infty} d\omega \frac{\tilde{r}''(\omega)}{\omega} \quad (\text{B3})$$

where  $P$  denotes the principal part of and where it has been assumed that there is negligible absorption in the frequency interval  $(\omega_{\text{v}}, \omega_{\text{el}})$ , so  $\tilde{r}''(\omega)$  is practically zero there. In obtaining eq B3, the large separation of the two frequency regions in the integrations allows us to assume  $\omega_{\text{v}} \ll \omega_{\text{op}} \ll \omega_{\text{el}}$ , and so  $\omega_{\text{op}}^2$  and  $\omega^2$  dominate in the denominators of the first and second integrals, respectively, in eq B2).

If the upper limit in eq B1 were replaced by  $\omega_{\text{op}}$ , it would become

$$- \frac{2\Delta\mu^2}{\pi} \int_0^{\omega_{\text{op}}} d\omega \frac{\tilde{r}''(\omega)}{\omega} = - \frac{2\Delta\mu^2}{\pi} \left( \int_0^{\infty} d\omega \frac{\tilde{r}''(\omega)}{\omega} - \int_{\omega_{\text{op}}}^{\infty} d\omega \frac{\tilde{r}''(\omega)}{\omega} \right) = \Delta\mu^2(r_{\text{s}} - r_{\text{op}}) \quad (\text{B4})$$

where we have used eqs B1 and B3.

Thus, in  $\Delta E(t)$ , there is expected to be an initial drop that is faster than the time resolution set by this cutoff frequency  $\omega_{\text{op}}$ , due to the electronic polarization:

$$\Delta E(t=0^+) = -\Delta\mu^2 r_{\text{op}} \quad (\text{B5})$$

We see from the above equation that when the  $\Delta E(t)$  is calculated using  $\omega_{\text{op}}$  instead of  $\infty$  in eq (A6) as the upper limit of integration, the  $\Delta E(t)$  starts from a value  $\Delta E(0^+)$  that arises from the electronic polarization.  $\Delta E(t)$  eventually goes to a static interaction energy,  $\Delta E(t \rightarrow +\infty)$ , which equals  $-\Delta\mu^2 r_{\text{s}}$  (eq A6). Thus, the changes in  $\Delta E(t)$  after the initial brief time interval,  $0^+$ , describe the solvational energy that arises from the nuclear response of the solvent.

## References and Notes

- (1) Nee, T.-W.; Zwanzig, R. *J. Chem. Phys.* **1970**, *52*, 6353. van der Zwan, G.; Hynes, J. T. *J. Chem. Phys.* **1982**, *76*, 2993.
- (2) Ware, W. R.; Lee, S. K.; Brant, G. J.; Chow, P. P. *J. Chem. Phys.* **1971**, *54*, 4729. Okamura, T.; Sumitani, M.; Yoshihara, K. *Chem. Phys. Lett.* **1983**, *94*, 339. Su, S.-G.; Simon, J. D. *J. Phys. Chem.* **1987**, *91*, 2693.
- (3) Jarzēba, W.; Walker, G. C.; Johnson, A. E.; Kahlow, M. A.; Barbara, P. F. *J. Phys. Chem.* **1988**, *92*, 7039.
- (4) Maroncelli, M.; Fleming, G. R. *J. Chem. Phys.* **1987**, *86*, 6221.
- (5) Horng, M. L.; Gardecki, J. A.; Papazyan, A.; Maroncelli, M. *J. Phys. Chem.* **1995**, *99*, 17311. Gardecki, J.; Horng, M. L.; Papazyan, A.; Maroncelli, M. *J. Mol. Liq.* **1995**, *65*–6, 49.
- (6) Maroncelli, M. Continuum Estimates of Rotational Dielectric Friction and Polar Solvation. *J. Phys. Chem.*, in press. Kumar, P. V.; Maroncelli, M. *J. Chem. Phys.* **1995**, *103*, 3038.
- (7) Jimenez, R.; Fleming, G. R.; Kumar, P. V.; Maroncelli, M. *Nature* **1994**, *369*, 471.
- (8) Jarzēba, W.; Walker, G. C.; Johnson, A. E.; Barbara, P. F. *Chem. Phys.* **1991**, *152*, 57.

- (9) Maroncelli, M.; Castner, E. W., Jr.; Bagchi, B.; Fleming, G. R. *Faraday Discuss. Chem. Soc.* **1988**, *85*, 199.
- (10) Castner, E. W., Jr.; Fleming, G. R.; Bagchi, B. *Chem. Phys. Lett.* **1988**, *143*, 270.
- (11) Wolynes, P. G. *J. Chem. Phys.* **1987**, *86*, 5133. Rips, I.; Klafter, J.; Jortner, J. *J. Chem. Phys.* **1988**, *88*, 3246. *Ibid.* **1988**, *89*, 4288. Nichols, A. L., III; Calef, D. F. *J. Chem. Phys.* **1988**, *89*, 3783.
- (12) Raineri, F. O.; Resat, H.; Perng, B.-C.; Hirata, F.; Friedman, H. L. *J. Chem. Phys.* **1994**, *100*, 1477. Zhou, Y.; Friedman, H. L.; Stell, G. *J. Chem. Phys.* **1989**, *91*, 4885. Fried, L. E.; Mukamel, S. *J. Chem. Phys.* **1990**, *93*, 932. Loring, R. F.; Mukamel, S. *J. Chem. Phys.* **1987**, *87*, 1272. Bagchi, B.; Chandra, A. *J. Chem. Phys.* **1989**, *90*, 7338.
- (13) Maroncelli, M.; Fleming, G. R. *J. Chem. Phys.* **1988**, *89*, 875.
- (14) Kahlow, M. A.; Jarzēba, W.; Kang, T. J.; Barbara, P. F. *J. Chem. Phys.* **1989**, *90*, 151.
- (15) Bagchi, B.; Chandra, A. *Adv. Chem. Phys.* **1991**, *80*, 1. Bagchi, B. *Annu. Rev. Phys. Chem.* **1989**, *40*, 115.
- (16) Roy, S.; Bagchi, B. *J. Chem. Phys.* **1993**, *99*, 9938.
- (17) Nandi, N.; Roy, S.; Bagchi, B. *J. Chem. Phys.* **1995**, *102*, 1390.
- (18) Gertner, B. J.; Whitnell, R. M.; Wilson K. R.; Hynes, J. T. *J. Am. Chem. Soc.* **1991**, *113*, 74.
- (19) Maroncelli, M.; Fleming, G. R. *J. Chem. Phys.* **1988**, *89*, 5044.
- (20) Ladanyi, B. M.; Stratt, R. M. *J. Phys. Chem.* **1995**, *99*, 2502; *Ibid.* **1996**, *100*, 1266.
- (21) Cho, M.; Rosenthal, S. J.; Scherer, N. F.; Ziegler, L. D.; Fleming, G. R. *J. Chem. Phys.* **1992**, *96*, 5033.
- (22) Song, X.; Marcus, R. A. *J. Chem. Phys.* **1993**, *99*, 7768.
- (23) Hasted, J. B. *Aqueous Dielectrics*; Chapman and Hall: London, 1973.
- (24) Asfar, M. N.; Hasted, J. B. *Infrared Phys.* **1978**, *18*, 835. Hasted, J. B.; Husain, S. K.; Frescura, F. A. M.; Birch, J. R. *Infrared Phys.* **1987**, *27*, 11. Hale, G. M.; Query, M. R. *Appl. Opt.* **1973**, *12*, 555.
- (25) Böttcher, C. J. F. *Theory of Electric Polarization*; Elsevier: Amsterdam, 1983; Vol. 1.
- (26) Onsager, L. *J. Am. Chem. Soc.* **1936**, *58*, 1486.
- (27) For example: Mathews, J.; Walker, R. L. *Mathematical Methods of Physics*, 2nd ed.; W. A. Benjamin: New York, 1970; pp 246–247. Titchmarsh, E. C. *Introduction to the Theory of Fourier Integrals*, 2nd ed.; The Clarendon Press: Oxford, 1948; pp 4–6.
- (28) For example: Kubo, R.; Toda, M.; Hashitsume, N. *Statistical Physics*; Springer-Verlag: New York, 1983; Vol. II, p 120. Ginzburg, V. L. *The Propagation of Electromagnetic Waves in Plasmas*, 2nd ed.; Pergamon Press: Oxford, 1970; pp 4–7.
- (29) For example: Jackson, J. D. *Classical Electrodynamics*, 2nd ed.; Wiley: New York, 1975.
- (30) Since all the time-dependent physical quantities,  $\mathbf{P}(\mathbf{r}, t)$ ,  $\mathbf{E}(\mathbf{r}, t)$ , and  $\mathbf{D}(\mathbf{r}, t)$ , are real,  $\alpha_i(t)$  is also real. Thus, when  $z = \omega$ , a real variable, the Fourier transform  $\tilde{\alpha}_i(\omega)$  has the property,  $\tilde{\alpha}_i(-\omega) = \tilde{\alpha}_i^*(\omega)$ , where  $\tilde{\alpha}_i^*$  is the complex conjugate of  $\tilde{\alpha}_i$ . From eqs 13 and 14, it is also true that  $\epsilon_i(-\omega) = \epsilon_i^*(\omega)$  and  $r(-\omega) = r^*(\omega)$ .
- (31) Bagchi, B.; Oxtoby, D. W.; Fleming, G. R. *Chem. Phys.* **1984**, *86*, 257.
- (32) We note, from eq (5), that  $\tilde{r}(0) = \int_{-\infty}^{\infty} r(t) dt = \int_0^{\infty} r(t) dt$  since  $r(t) = 0$  for  $t < 0$  and note that  $\int_{-\infty}^t r(t-t') dt' = \int_0^{\infty} r(t') dt'$ . Also,  $\tilde{r}(0)$  is a real number since  $r(t)$  is a real function of  $t$ .
- (33) Since  $r(t)$ , the response function, goes to zero exponentially as  $t$  goes to  $+\infty$ , and it equals zero for negative  $t$ 's (causality), its corresponding transform  $\tilde{r}(z)$  is analytic both on the real axis and in the lower half complex plane of  $z$  (cf. eq 5).
- (34) Osborn, J. A. *Phys. Rev.* **1945**, *67*, 351. Stoner, E. C. *Phil. Mag.* **1945**, *36*, 803.
- (35) In ref 22 the boundary used for switching from Debye's formula to the spline fit was  $1.0 \times 10^{11}$  rad  $s^{-1}$ . Changing that number to the current  $3.0 \times 10^{11}$  rad  $s^{-1}$  does not change the result of the calculation presented in this work.
- (36) Song, X.; Chandler, D.; Marcus, R. A. *J. Phys. Chem.* **1996**, *100*, 11954.
- (37) For example: McQuarrie, D. A. *Statistical Mechanics*; Harper & Row: New York, 1976; pp 498–499.
- (38) Böttcher, C. J. F.; Bordewijk P. *Theory of Electric Polarization*; Elsevier: Amsterdam, 1973; Vol. 2.
- (39) Loring, R. F.; Yan, Y. J.; Mukamel S. *J. Chem. Phys.* **1987**, *87*, 5840.
- (40) van der Zwan, G.; Hynes, J. T. *J. Phys. Chem.* **1985**, *89*, 4181.
- (41) Neumann, M. *J. Chem. Phys.* **1986**, *85*, 1567.